

Adaptive Optics in Star Formation

Wolfgang Brandner

*Max-Planck-Institut für Astronomie, Königstuhl 17, D-69117
 Heidelberg, Germany*

Abstract. Over the past ten years, the concept of adaptive optics has evolved from early experimental stages to a standard observing tool now available at almost all major optical and near-infrared telescope facilities. Adaptive optics will also be essential in exploiting the full potential of the large optical/infrared interferometers currently under construction. Both observations with high-angular resolution and at high contrast, and with a high point source sensitivity are facilitated by adaptive optics. Among the areas which benefit most from the use of adaptive optics are studies of the circumstellar environment (envelopes, disks, outflows), substellar companions and multiple systems, and dense young stellar populations. This contribution highlights some of the recent advances in star formation studies facilitated by adaptive optics, and gives a brief tutorial on optimized observing and data reduction strategies.

1. AO - (emerging) main-stream observing technique for SF studies

More than twenty contributions to IAU Symp. 221 (many of which can be found in the present proceedings) are based at least in part on observations with ground-based telescopes equipped with Adaptive Optics (AO). Hence it is fair to say that AO has already been adopted as a main-stream observing technique for high-resolution star formation (SF) studies. The SF research topics addressed by AO observations range from studies of young substellar companions and the circumstellar environment of young stars (disks & outflows), over studies of sub-stellar and stellar binaries, to studies of massive star forming sites and environments (including Galactic and extra-galactic starbursts).

2. AO Basics: Observing facilities & glossary of AO terms

2.1. Observing facilities

AO is the real-time measurement and correction of the effect of atmospheric turbulence on an electromagnetic wavefront from a distant (astronomical) source. The temporal stability of an AO correction facilitates long integration times, and hence increases the limiting sensitivity of any detector system with a finite read-noise. By now, many of the 3m- to 10m-class optical/NIR telescopes are equipped with AO. Astronomical AO systems are using Shack-Hartmann-, Curvature- or Pyramid-type wavefront sensors with 19 to ≈ 1000 sensing ele-

ments, and deformable mirrors with a corresponding number of actuators. Wavefront sensing is in general done in the optical, though some of the newer systems are capable of sensing low-order tip-tilt aberrations also in the near-infrared, and at least one system (NACO at the ESO VLT) is equipped with a full-fledged NIR wavefront sensor. Science instruments in general cover the wavelength range from 1 to $5\mu\text{m}$, and typical instrument modes cover direct imaging, polarimetry, long-slit and integral field spectroscopy (including scanning Fabry-Perots), coronagraphy, and differential imaging.

2.2. Brief Glossary of AO related & relevant terms

Since AO systems do a real-time analysis and compensation of atmospheric wavefront aberrations, the properties of the correction, and hence the quality of the science image, vary as a function of atmospheric (turbulence) parameters. A basic understanding of the physical parameters characterising the atmospheric turbulence and the (instrumental) limitation of a given AO system is a prerequisite for designing successful AO observing runs, and for devising an optimized data reduction and analysis strategy.

Definitions of common AO terms:

- **Strehl ratio (SR):** the ratio between the peak flux of an observed point-spread function (PSF) and a perfect (diffraction limited) PSF normalized to the same flux
- **Fried parameter:** r_0 corresponds to the size of the atmos. turbulence cell projected to the ground layer. It scales with wavelength as $r_0 \propto \lambda^{6/5}$
- **Seeing angle:** It is defined as $\beta = \lambda/r_0 \propto \lambda^{-1/5}$ (0.5'' seeing at $\lambda = 500\text{ nm}$ corresponds to $r_0 = 0.2\text{ m}$)
- **Coherence time:** τ_0 is the lifetime of (atmospheric) speckles. It scales with wavelength as $\tau_0 \propto \lambda^{6/5}$
- **Isoplanatic Angle:** Θ_0 is the angular distance from the reference source used for wavefront sensing, at which the Strehl ratio drops by $1/e$. It scales with wavelength as $\Theta_0 \propto \lambda^{6/5}$ (i.e., an isoplanatic angle size of $3''$ at a wavelength of 500 nm corresponds to $\Theta = 18''$ at $\lambda = 2.2\mu\text{m}$)

It is important to keep in mind that the atmospheric turbulence properties r_0 , τ_0 , and Θ_0 can vary independently of each other. In particular, β and Θ_0 may originate in different layers of the atmosphere. In general, observations at longer wavelengths benefit from better seeing (β) and longer coherence time (τ_0), and hence result in a better AO correction and higher Strehl ratio.

2.3. How to design a successful AO observing run

The four main ingredients for designing and executing a successful AO observing run are **i) Select a bright, compact reference source:** NACO at the ESO VLT, e.g., gives partial correction for reference sources as faint as $V \leq 17\text{ mag}$, but full AO correction requires $V \leq 12\text{ mag}$. In the limit, only low-order aberration like tip-tilt are corrected, resulting in a low SR. **ii) Small angular separation**

between the reference source and the science target (i.e. within the isoplanatic angle) is mandatory to achieve at least 37% ($1/e$) of the on-axis SR. **iii) Good atmospheric conditions** (large r_0 , τ_0) become increasingly important for observations at shorter wavelengths (going from $\dots \rightarrow L \rightarrow K \rightarrow H \rightarrow J \rightarrow Z \rightarrow I \rightarrow \dots$). Hence it is advisable to choose service mode observations wherever this mode is offered. and **iv) A Reference PSF** is important for the interpretation of AO observations of extended sources, and for high-contrast applications.

2.4. AO specific effects to watch out for during data reduction

AO data are subject to angular and temporal variations of the PSF, as well as differential atmospheric refraction, which at 8 m- to 10 m-class telescopes can be of the same order of magnitude as the diffraction limited PSF size.

Temporal PSF variations Temporal variations of the PSF imply that the quality of individual science frames has to be checked before combining or averaging the frames, and that in particular in the case of marginal data, an image selection has to be applied (Tessier et al. 1994). In crowded stellar fields, the angular variation of the PSF can be measured and modelled, and then taken into account in the course of the data analysis (e.g., using a linearly varying PSF in DAOPHOT, or the new implementation of the StarFinder code). In the case of morphological studies of extended sources like deeply embedded Young Stellar Objects, galaxy clusters, and lensing studies, a knowledge of the atmospheric turbulence profile is required for a proper interpretation of the data. Current AO systems are not well suited for “wide-field” morphological studies. These studies therefore have to be deferred until multi-conjugated AO (MCAO) systems become operational.

Speckle noise and high-contrast AO AO systems operate in a “closed-loop” configuration. The wavefront sensor signal corresponds to an error signal, i.e., the difference between the corrections applied by the deformable mirror and the actual wavefront distortion. Since AO systems can only partially correct the wavefront errors, a residual noise component (“speckle noise”) remains in the corrected PSF. Because of the nature of the AO correction, this speckle noise does not arise from statistically independent photons. Instead, speckle-noise constitutes a correlated noise component, which is the limiting factor for high-contrast observations (see Racine et al. 1999, and references therein). Figure 1 shows an example of the effect of speckle noise. It was obtained during a lab experiment with a turbulence simulator and the VLT adaptive optics system NACO. In the top left and right of Figure 1, two subsequent images of a point source, which was imaged through the turbulence simulator, and then AO corrected and observed, are displayed. In the lower left, the difference between the two images on the top is shown. Despite the fact that the “observing conditions” (r_0 , τ_0) were kept constant, strong residuals due to the speckle noise can be observed.

The concept of differential imaging One way to reduce the residuals is the method of dual- (or differential-) imaging. Here, two images (either in two orthogonal polarization states – see Kuhn et al. 2001; Potter 2003 – or in two neighbouring wavelength regions – see Racine et al. 1999; Marois et al. 2000) have

to be obtained simultaneously. By taking the difference of these two images, the photons from the bright star (which does not exhibit a high degree of polarization or strong wavelength dependent spectral features) effectively cancel out, while the much fainter signal from, e.g., a circumstellar disk (seen in scattered, i.e., polarized light) or a substellar companion (with strong molecular absorption bands) clearly stands out. In the lower right panel of Figure 1 the reduced residuals are apparent (Brandner & Potter 2002).

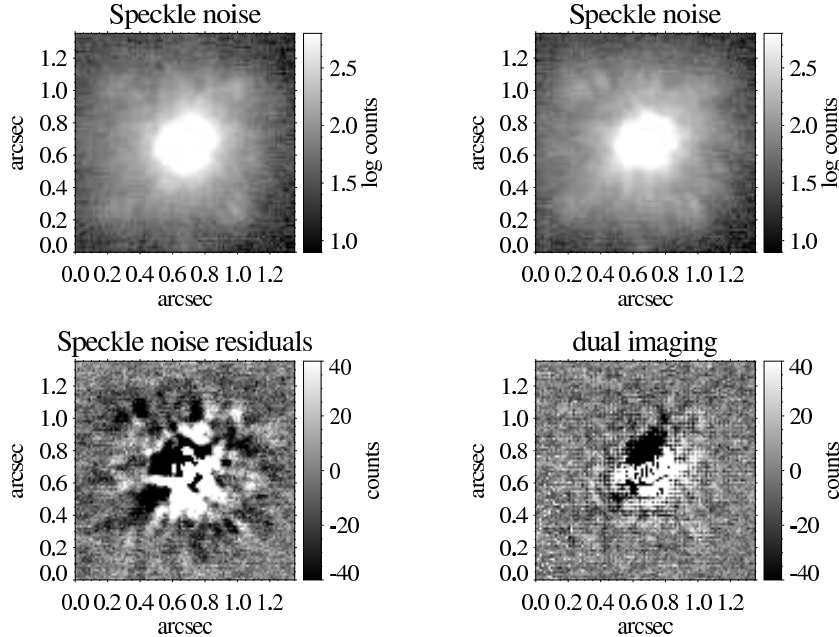


Figure 1. Examples of speckle noise, and the gain in noise suppression by using dual imaging with a Wollaston prism (lab experiment using the VLT AO system NAOS & CONICA).

As an example, we show in Figure 2 the brown dwarf Gl 229b. On the top, the near infrared spectrum obtained by Oppenheimer et al. (1995) is plotted. The shape of the spectral energy distribution is dominated by strong molecular absorption bands and the intermittent pseudo-continuum. In the H-band, such an intermittent pseudo-continuum is located between water and ammonia absorption bands at wavelengths $\leq 1.58 \mu\text{m}$, and a methane absorption band at wavelengths $\geq 1.61 \mu\text{m}$. In the lower half of Figure 2 narrow-band imaging data on Gl 229b as obtained with the AO system ADONIS at the ESO 3.6m telescope in 1997 is shown. A circular variable filter was used to scan through different wavelength ranges. As is apparent from the images, Gl 229b is 2 mag brighter at a wavelength of $\approx 1.57 \mu\text{m}$ than at the wavelength of neighbouring molecular absorption bands (see Rosenthal et al. 1996).

Spectral Differential Imagers For CONICA, the Spectral Differential Imager (SDI) upgrade (led by R. Lenzen at MPA & L. Close at Steward Obs.) consists of a four-channel beamsplitter combined with a quad-filter. Two of the quadrants of the quad-filter are adjusted to the longest wavelength located in

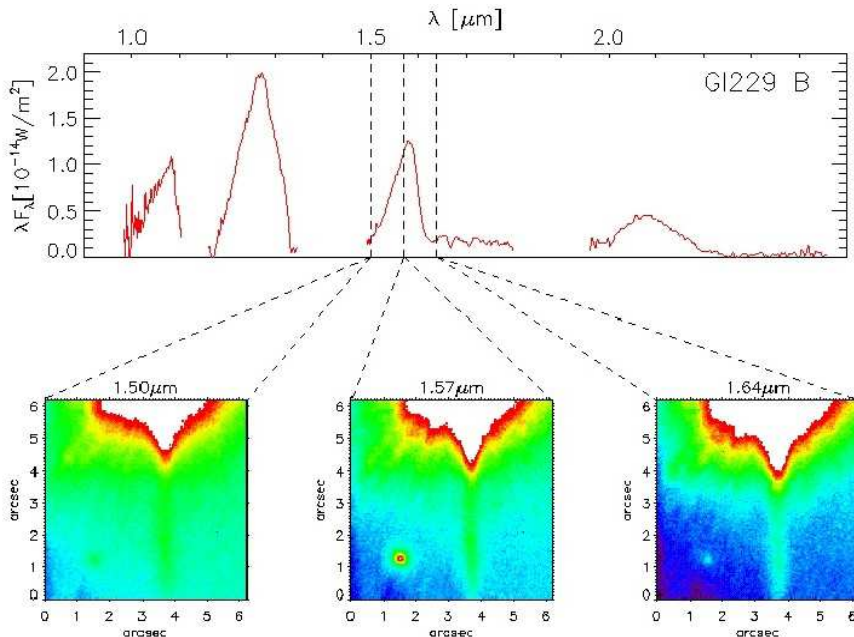


Figure 2. Top: Low-resolution spectrum from the data presented in the discovery paper on Gl 229B by Oppenheimer et al. (1995). Bottom: Gl 229 B observed with the adaptive optics system ADONIS at the ESO 3.6m telescope with a circular variable filter centered on absorption bands and in the continuum (Brandner et al. 1998). In the “continuum” ($1.57 \mu\text{m}$), Gl 229 B is about 2 mag brighter than at neighbouring wavelengths ($\approx 1.64 \mu\text{m}$) in a strong CH_4 absorption band.

a Methane absorption band at $1.625 \mu\text{m}$, while the other two quadrants transmit light at $1.600 \mu\text{m}$ (location of pseudo-continuum emission) and at $1.575 \mu\text{m}$ (location of a potential ammonia absorption band), respectively. The final differential image is obtained by rescaling, interpolation and subtraction, similar to the procedure outlined by Marois et al. (2000). The implementation of the SDI mode, and the first on-sky tests with NACO at the VLT were carried out in August 2003, and a brightness contrast ratio of 5×10^4 at a separation of $0.5''$ from a bright reference source was achieved. One of the science goals of the CONICA Planet Finder upgrade is to detect giant planets with masses down to $\approx 5 M_{\text{Jup}}$ around nearby young stars.

Atmospheric refraction and spectroscopy Differential atmospheric dispersion leads to elongated (spectrally spread) PSFs. It scales with the airmass and the overall atmospheric conditions (see Table 1). For broad-band imaging applications, the apparent positions of blue and red objects are shifted with respect to each other along the parallactic angle. This effect, when not corrected for, limits the accuracy of relative astrometric measurements. Spectroscopy with a narrow slit (width close to the diffraction limit), which is not aligned with the parallactic angle, results in a wavelength dependent loss of light. It is impor-

Table 1. Differential atmospheric refraction in mas in the JHK bands for median atmospheric conditions at Paranal ($T = 11.5$ C, $P = 743$ hPa, relative humidity 15%). For comparison, the diffraction limit of an 8m-telescope is given in the last row.

wavelength [μm]	1.15–1.35	1.55–1.80	2.05–2.35
zenith distance	[mas]	[mas]	[mas]
10°	9	4	2
20°	18	9	5
30°	28	15	8
40°	41	21	11
50°	59	30	16
60°	85	44	23
FWHM ($1.22\lambda/D$)	38	52	68

tant to keep this in mind when trying to do spectro-photometry. A much more thorough discussion of the particular effects of long-slit spectroscopy combined with adaptive optics is presented by Goto (2004). Many of these effects can also be avoided by employing filled aperture integral field spectrographs instead of long-slit spectrographs.

3. Science Examples

Science studies of star forming environments can be sub-divided into two major categories: high-resolution and high-contrast studies of the immediate environment of a (bright) source, and high-resolution “wide-field” studies of a complex or crowded environment. In the following, a brief – and necessarily incomplete – summary of star formation studies with AO is presented.

3.1. “Wide-field” AO ($\emptyset \leq 20''$)

Studies of stellar populations in crowded fields require high-angular resolution. One area of particular interest is the mass function of Galactic and extra-galactic starburst clusters. Examples of starburst clusters studied with AO include R136 in the 30 Doradus region in the Large Magellanic Cloud (Brandl et al. 1996), the central cluster of the giant HII region NGC 3603 in the Carina spiral arm (Eisenhauer et al. 1998), and the Arches cluster in the Galactic Center region (Blum et al. 2001, Stolte et al. 2002, Yang et al. 2002).

Figure 3, taken from Stolte et al. (2003), shows a comparison of ground- and space based NIR observations of the Arches cluster. In the case of low Strehl ratios (left), crowding limits the sensitivity towards faint point sources. The colour-magnitude diagram on the right is based on data with moderate SR of 14% in H, and 20% in K, and clearly demonstrate that ground-based AO at 8 m-class telescopes can be superior to HST/NICMOS (middle panel). The Orion star forming region has also been studied with AO, in particular the stellar

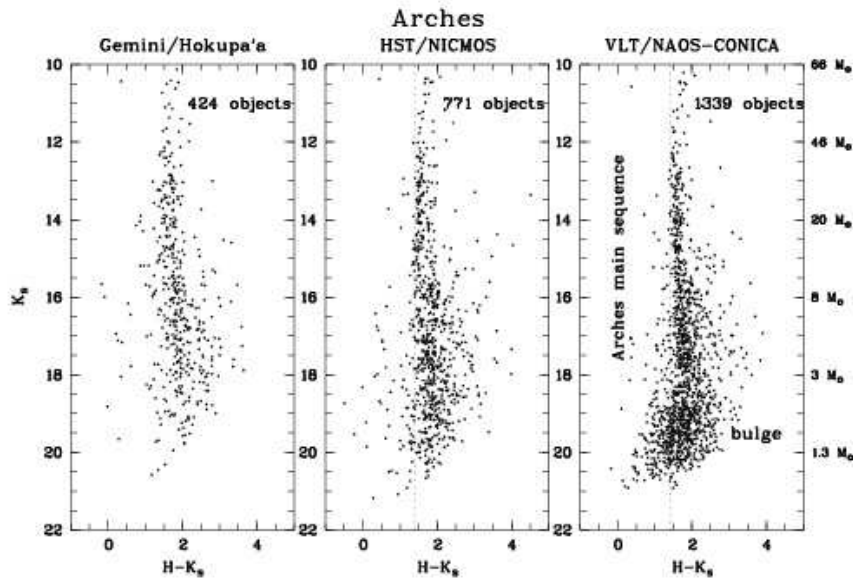


Figure 3. K vs. H-K colour-magnitude diagrams for the Arches cluster as obtained with the low-order curvature AO system Hokupa'a at Gemini North, NICMOS aboard HST, and the intermediate order Shack-Hartmann AO system NACO at the ESO VLT (Stolte et al. 2003).

population in the central core of the Trapezium cluster (Simon et al. 1999), photoevaporating stellar envelopes (McCullough et al. 1995), and the complex interstellar environment in the vicinity of the BN/KL object (e.g., Vannier et al. 2001).

3.2. High-contrast AO (Contrast $\geq 10^5$)

Despite the above mentioned limitations due to PSF variations and speckle noise, AO has been very successfully employed to study the close environment of young stellar objects. This includes both a search for faint point sources like substellar companions, and for faint extended emission from circumstellar disks, envelopes and outflows. Stellar companions to young stars like NX Pup (Brandner et al. 1995), VW Cha (Brandeker et al. 2001), HD 98800 (Prato et al. 2001), χ 1 Orionis (König et al. 2002) or TY CrA (Chauvin et al. 2003) have been identified by means of AO. Liu et al. (2002), e.g., detected a substellar (spectral type L) companion to the young solar analog HR 7672 (see Figure 4), and a binary brown dwarf companion to the young star HD 130948 was identified by Potter et al. (2002) and Goto et al. (2002). Systematic studies of the binary content of star forming regions like IC 348 (Duchêne et al. 1999), the Pleiades (Martín et al. 2000), NGC 6611 (Duchêne et al. 2001), MBM 12 (Chauvin et al. 2002), NGC 2024 (Beck et al. 2003) have been carried out as well.

Jets and outflows from young stars were studied by Dougados et al. (2000), Millan-Gabet & Monnier (2002), and López-Martin et al. (2003). Ultra-compact

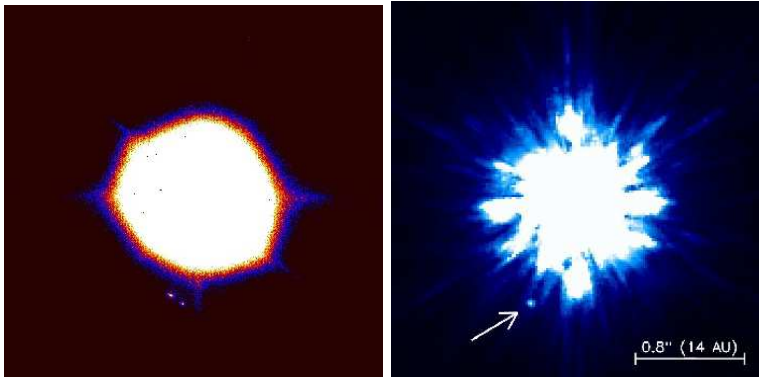


Figure 4. Faint companions and companion candidates: The Palomar AO system (left) detected this binary companion candidate, which has a separation of $5''$, and is about 13 mag fainter in K than the primary (courtesy of Matthew Britton, Caltech). Using the Keck AO system (right), Liu et al. (2002) detected an L-dwarf companion to the young solar analog HR 7672. The companion is at a separation of $0.79''$, and 8.6 mag fainter than the primary in K-band.

H II regions are studied, e.g., by Feldt et al. (1999) and Henning et al. (2001). Quite a number of AO studies also concentrated on the properties of circumstellar disks around young stars such as GG Tau (Roddier et al. 1996, Itoh et al. 2002), HD 100546 (Pantin et al. 2000), UY Aur (Potter et al. 2000), LkH α 198 (Fukagawa et al. 2002), HD 141569 (Boccaletti et al. 2003), HD 150193 A (Fukagawa et al. 2003), HV Tauri C (Stapelfeldt et al. 2003), or led to the detection of edge-on disks, like, e.g., in MBM 12 (Jayawardhana et al. 2002), or around HV Tau C (Monin & Bouvier 2000).

3.3. Spectroscopy with AO

T Tauri itself has been the focus of near-infrared spectroscopic studies combined with adaptive optics in the past couple of years. Kasper et al. (2002) obtained H- and K-band spectra of the main components T Tauri North and South using the Calar Alto 3.5 m telescope with its AO system ALFA, while Duchêne et al. (2002) took K-band spectra of the two components comprising the close binary T Tauri South A&B using the Keck AO system. Using the PUEO system at CFHT, Garcia et al. (1999) obtained spatially resolved spectroscopy of the Z CMa components. Davies et al. (2001) studied young stellar objects in LkH α 225 by means of AO integral field spectroscopy with the ALFA system on Calar Alto.

3.4. Interferometry and AO

Both the Keck and the VLT Interferometer are now equipped with AO systems. The first science results obtained on the circumstellar disk around DG Tau have just been published (Colavita et al. 2003, see also Akeson, these proceedings), and many more results are expected for the near future.

4. Further Reading

For further reading, the following online references on the theory and application of adaptive optics are recommended:

- AO Lecture by Laird Close:
http://athene.as.arizona.edu/~lclose/a519/Lecture_1.html
- AO Lecture by Claire Max: <http://cfao.ucolick.org/~max/289C>
- (Theory of) AO tutorial by Andrei Tokovinin:
<http://www.ctio.noao.edu/~atokovin/tutorial/intro.html>
- AO: Past, Present and Future by Olivier Lai:
http://www.cfht.hawaii.edu/Instruments/Imaging/AOB/local_tutorial.html

References

- Beck, T.L., Simon, M., Close, L.M. 2003, ApJ 583, 358
- Blum, R.D., Schaerer, D., Pasquali, A. et al. 2001, AJ 122, 1875
- Boccaletti, A., Augereau, J.C., Marchis, F., Hahn, J. 2003, ApJ 585, 494
- Brandeker, A., Liseau, R., Artymowicz, P., Jayawardhana, R. 2001, ApJ 561, L199
- Brandl, B., Sams, B.J., Bertoldi, F. et al., 1996, ApJ 466, 254
- Brandner, W., Bouvier, J., Grebel, E., Tessier, E., De Winter, D., Beuzit, J. 1995, A&A 298, 818
- Brandner, W., Frink, S., Köhler, R., Kunkel, M. 1998, in *10th Cambridge Workshop on Cool Stars, Stellar Systems and the Sun*, eds. R.A. Donahue & J.A. Bookbinder, ASP Conf. Ser. 154, p. 1836
- Brandner, W., Potter, D. 2002, in *Scientific Drivers for ESO Future VLT/VLTI Instrumentation*, eds. J. Bergeron & G. Monnet (Berlin: Springer-Verlag), 264
- Chauvin, G., Ménard, F., Fusco, T. et al. 2002, A&A 394, 949
- Chauvin, G., Lagrange, A.-M., Beust, H. et al. 2003, A&A 406, L51
- Colavita, M., Akeson, R., Wizinowich, P. et al. 2003, ApJ 592, L83
- Davies, R.I., Tecza, M., Looney, L.W. et al. 2001, ApJ 552, 692
- Dougados, C., Cabrit, S., Lavalley, C., Ménard, F., 2000, A&A 357, L61
- Duchêne, G., Bouvier, J., Simon, T. 1999, A&A 343, 831
- Duchêne, G., Simon, T., Eisloffel, J., Bouvier, J. 2001, A&A 379, 147
- Duchêne, G., Ghez, A.M., McCabe, C. 2002, ApJ 568, 771
- Eisenhauer, F., Quirrenbach, A., Zinnecker, H., Genzel, R. 1998, ApJ 498, 278
- Feldt, M., Stecklum, B., Henning, T., Launhardt, R., Hayward, T.L. 1999, A&A 346, 243
- Fukagawa, M., Tamura, M., Suto, H. et al. 2002, PASJ 54, 969
- Fukagawa, M., Tamura, M., Itoh, H. et al. 2003, ApJ 590, L49
- Garcia, P.J.V., Thiebaud, E., Bacon, R. 1999, A&A 346, 892

- Goto, M., Kobayashi, N., Teradam H. et al. 2002, ApJ 567, L59
- Goto, M. 2004, in *ESO workshop on "Science with Adaptive Optics"*, eds. W. Brandner & M. Kasper (Berlin: Springer-Verlag), in press
- Henning, T., Feldt, M., Stecklum, B., Klein, R. 2001, A&A 370, 100
- Jayawardhana, R., Luhman, K.L., D'Alessio, P., Stauffer, J.R. 2002, ApJ 571, L51
- Kasper, M.E., Feldt, M., Herbst, T.M., Hippler, S., Ott, T., Tacconi-Garman, L.E. 2002, ApJ 568, 267
- König, B., Fuhrmann, K., Neuhäuser, R., Charbonneau, D., Jayawardhana, R. 2002, A&A 394, L43
- Kuhn, J.R., Potter, D., Parise, B. 2001, ApJ 553, L189
- Liu, M.C., Fischer, D.A., Graham, J.R., Lloyd, J.P., Marcy, G.W., Butler, R.P. 2002, ApJ 571, 519
- López-Martin, L., Cabrit, S., Dougados, C. 2003, A&A 405, L1
- Marois, C., Doyon, R., Racine, R., Nadeau, D. 2000, PASP 112, 91
- Martín, E.L., Brandner, W., Bouvier, J. et al. 2000, ApJ 543, 299
- McCullough, P.R., Fugate, R.Q., Christou, J.C. et al. 1995, ApJ 438, 394
- Millan-Gabet, R., Monnier, J.D. 2002, ApJ 580, L167
- Monin, J.-L., Bouvier, J. 2000, A&A 356, L75
- Oppenheimer, B.R., Kulkarni, S.R., Matthews, K., Nakajima, T. 1995, Science 270, 1478
- Pantin, E., Waelkens, C., Lagage, P.O. 2000, A&A 361, L9
- Potter, D.E., Close, L.M., Roddier, F. et al. 2000, ApJ 540, 422
- Potter, D., Martín, E.L., Cushing, M.C., Baudoz, P., Brandner, W., Guyon, O., Neuhäuser, R. 2002, ApJ 567, L133
- Prato, L., Ghez, A.M., Piña, R.K. et al. 2001, ApJ 549, 590
- Racine, R., Walker, G.A.H., Nadeau, D., Doyon, R., Marois, C. 1999, PASP 111, 587
- Roddier, F., Roddier, C., Northcott, M.J., Graves, J.E., Jim, K. 1996, ApJ 463, 326
- Rosenthal, E.D., Gurwell, M.A., Ho, P.T.P. 1996, Nature 384, 243
- Simon, M., Close, L., Beck, T.L. 1999, AJ 117, 1375
- Stapelfeldt, K.R., Ménard, F., Watson, A.M. et al. 2003, ApJ 589, 410
- Stolte, A., Grebel, E., Brandner, W., Figer, D. 2002, A&A 394, 459
- Stolte, A., Brandner, W., Grebel, E., Figer, D.F. et al. 2003, The Messenger No. 111, p. 9
- Tessier, E., Bouvier, J., Beuzit, J.-L., Brandner, W. 1994, The Messenger No. 78, p. 35
- Vannier, L., Lemaire, J.L., Field, D., Pineau des Forets, G., Pijpers, F.P., Rouan, D. 2001, A&A 366, 651
- Yang, Y., Park, H.S., Lee, M.G., Lee, S.-G. 2002, JKAS 35, 131